

# 1 **Microtiter plate-based antibody-competition assay to determine** 2 **binding affinities and plasma/blood stability of CXCR4 ligands**

3  
4  
5 Mirja Harms<sup>1</sup>, Andrea Gilg<sup>1</sup>, Ludger Ständker<sup>2</sup>, Ambros J. Beer<sup>3</sup>, Benjamin Mayer<sup>4</sup>, Volker  
6 Rasche<sup>5</sup>, Christian W. Gruber<sup>6</sup>, Jan Münch<sup>1,2\*</sup>

7  
8 <sup>1</sup> Institute of Molecular Virology, Ulm University Medical Center, Ulm, 89081, Germany

9 <sup>2</sup> Core Facility Functional Peptidomics, Ulm University Medical Center, Ulm, 89081,  
10 Germany

11 <sup>3</sup> Department of Nuclear Medicine, Ulm University Medical Center, Ulm, 89081, Germany

12 <sup>4</sup> Institute for Epidemiology and Medical Biochemistry, Ulm University, Ulm, 89081,  
13 Germany

14 <sup>5</sup> Experimental Cardiovascular Imaging (ExCaVI), Ulm University Medical Center, Ulm,  
15 89081, Germany

16 <sup>6</sup> Institute of Pharmacology, Center for Physiology and Pharmacology, Medical University of  
17 Vienna, 1090 Vienna, Austria

18  
19 \*Corresponding author: [jan.muench@uni-ulm.de](mailto:jan.muench@uni-ulm.de)  
20  
21

## 22 **ABSTRACT**

23  
24 C-X-C chemokine receptor type 4 (CXCR4) is involved in several intractable disease processes,  
25 including HIV infection, cancer cell metastasis, leukemia cell progression, rheumatoid arthritis,  
26 asthma and pulmonary fibrosis. Thus, CXCR4 represents a promising drug target and several  
27 CXCR4 antagonizing agents are in preclinical or clinical development. Important parameters  
28 in drug lead evaluation are determination of binding affinities to the receptor and assessment of  
29 their stability and activity in plasma or blood of animals and humans. Here, we designed a  
30 microtiter plate-based CXCR4 antibody competition assay that enables to measure inhibitory  
31 concentrations (IC<sub>50</sub> values) and affinity constants (K<sub>i</sub> values) of CXCR4 targeting drugs. The  
32 assay is based on the observation that most if not all CXCR4 antagonists compete with binding  
33 of the fluorescence-tagged CXCR4 antibody 12G5 to the receptor. We demonstrate that this  
34 antibody-competition assay allows a convenient and cheap determination of binding affinities  
35 of various CXCR4 antagonists in living cells within just 3 hours. Moreover, the assay can be  
36 performed in the presence of high concentrations of physiologically relevant body fluids, and  
37 thus is a useful readout to evaluate stability (i.e. half-life) of CXCR4 ligands in serum/plasma,  
38 and even whole human and mouse blood *ex vivo*. Thus, this optimized 12G5 antibody  
39 competition assay allows a robust and convenient determination and calculation of various  
40 important pharmacological parameters of CXCR4 receptor-drug interaction and may not only  
41 foster future drug development but also animal welfare by reducing the number of experimental  
42 animals.  
43  
44

## 45 Introduction

46

47 The G protein-coupled receptor CXCR4 (CXC chemokine receptor 4) is a 352 amino acid cell surface  
48 protein with CXCL12 as its sole endogenous chemokine ligand<sup>1,2,3</sup>. The CXCR4/CXCL12 pair plays an  
49 important and unique role in cellular trafficking processes involved in organ development,  
50 hematopoiesis, vascularization, in cell and tissue renewal and regeneration, in inflammation and immune  
51 control, stem cell homing and mobilization<sup>4,5,6,7,8</sup>. Aberrant CXCR4/CXCL12 signaling is associated  
52 with a variety of pathophysiological conditions including cancer metastasis, enhanced tumor growth,  
53 chronic inflammation, leukemia and altered immune responses<sup>9</sup>. Furthermore, CXCR4 is a major  
54 coreceptor of HIV-1 during the late stages of infection and associated with rapid disease progression<sup>10,11</sup>.  
55 Thus, CXCR4 represents an important drug target. Several small molecules (e.g. AMD3100<sup>12</sup>,  
56 AMD070<sup>13</sup>), peptides (e.g. Polyphemusin 2<sup>14</sup> or Ly2510924<sup>15</sup>), or nano- and antibodies (e.g.  
57 Ulocuplumab<sup>16</sup> or ALX-0651<sup>17</sup>) that target and antagonize CXCR4 have been identified<sup>9</sup> and represent  
58 promising leads for drug development. Diverse animal studies provided evidence that CXCR4 inhibitors  
59 allow mobilization of hematopoietic stem cells, suppression of CXCR4-tropic HIV-1 replication and  
60 reduction in tumor growth and/or metastasis. Several clinical studies that evaluate CXCR4 antagonists  
61 as therapeutic agents in e.g. pancreatic cancer, adenocarcinomas, multiple myeloma or myelokathexis  
62 are currently running. However, none of these compounds has been approved for the treatment of  
63 chronic diseases like cancer or HIV/AIDS. The main reason is likely because long-term inactivation of  
64 CXCR4 also inhibits the physiological function of the receptor and causes side effects<sup>18</sup>. The only  
65 licensed CXCR4 antagonist to date is AMD3100 (Plerixafor), which is used as single injection to  
66 mobilize hematopoietic stem cells in cancer patients<sup>9</sup>. AMD3100 is a bicyclam small molecule drug that  
67 was initially developed as a treatment against CXCR4-tropic HIV-1 infection but failed during long  
68 term application studies<sup>18,19</sup>. In the last years, several analogues of AMD3100 were developed covering  
69 a range of sub-structural types. One of them is the non-cyclam small molecule AMD070 that is orally  
70 bioavailable and was revived in several clinical trials including a phase III clinical trial for WHIM  
71 patients<sup>22,21</sup>. Another orally available small molecule is MSX-122 that was described as a partial  
72 antagonist of CXCR4 and is currently investigated in a phase II clinical trial as an oral drug for hot  
73 flashes in breast cancer-positive post-menopausal women<sup>20,21</sup>. Two other orally available small drug  
74 candidates are Burixafor (TG-0054) that is a monocyclic CXCR4 antagonist und currently tested in a  
75 phase II study for stem cell mobilization<sup>23,21</sup>, and the isothioureia compound IT1t that was used for  
76 crystallization of the CXCR4 receptor thereby revealing a distinct binding mode from AMD3100 within  
77 the receptor binding pocket<sup>24,25,26</sup>.

78

79 Besides small molecules, several peptide-based CXCR4 antagonist are also being tested for multiple  
80 applications. Those peptides are often based on naturally occurring ligands, e.g. the 17 amino acid  
81 CXCL12 analogue CTCE-9908<sup>27</sup>, and the two cyclic peptides LY2510924<sup>15</sup> and BKT-140<sup>28</sup> that are  
82 currently tested in phase II clinical trials determining their effect on different kinds of cancer and stem  
83 cell mobilization<sup>21,29</sup> (for a review see <sup>30</sup>). Another linear peptide drug candidate is EPI-X4 (Endogenous  
84 Peptide Inhibitor of CXCR4), a recently identified body own antagonist of CXCR4<sup>31,32,33</sup>. This 16-mer  
85 peptide encompasses residues 408-423 of human serum albumin and is proteolytically released from its  
86 precursor by acidic aspartic proteases<sup>34</sup>. EPI-X4 blocks CXCL12-mediated signaling, thereby  
87 preventing the migration of cancer cells, mobilizing hematopoietic cells and inhibiting inflammatory  
88 responses *in vitro* and in mouse models. In addition, EPI-X4 is also an effective inhibitor of CXCR4-  
89 tropic HIV-1. This endogenous peptide represents an interesting lead for further clinical development  
90 because it is not immunogenic and, in contrast to AMD3100, does not bind CXCR7<sup>31,35</sup>. In addition, it  
91 also acts as inverse agonist and reduces the basal signaling activity of CXCR4, and does not exert  
92 mitochondrial cytotoxicity. However, the short half-life of the peptide in plasma ( $t_{1/2} \sim 17$  min)<sup>31</sup> and its

93 only median potency in antagonizing CXCR4 (IC<sub>50</sub> to suppress CXCL12 migration in median  
94 micromolar range) prevent its further clinical development as CXCR4 targeting drug, at least for  
95 systematic therapy. A structure–activity relationship study allowed to reduce the size and to improve the  
96 CXCR4-antagonizing potency of EPI-X4<sup>31,36</sup>. One example of an optimized EPI-X4 derivative is  
97 WSC02 that encompasses only 12 residues and inhibits CXCR4-tropic HIV-1 infection and suppresses  
98 leukemia cell migration towards CXCL12 with IC<sub>50</sub> values in the nanomolar range. However, despite  
99 the improved CXCR4 antagonizing potency, EPI-X4 and its first-generation derivatives suffer from a  
100 low stability in plasma due to proteolytic inactivation of the peptide by leucyl aminopeptidases<sup>31,34</sup>.

101  
102 Proteolytic degradation often limits systemic therapeutic applications of peptide-based drugs. Increasing  
103 peptide stability relies often on evaluating large numbers of lead compounds, which requires suitable *in*  
104 *vitro* techniques providing reliable predictions of *in vivo* performance and reducing the number of animal  
105 experiments<sup>37</sup>. Peptide stability and proteolysis is usually determined *ex vivo* by spiking the peptide into  
106 plasma, serum or whole blood (derived from humans or mice), incubation at 37°C and subsequent  
107 analysis of the specimen by means of chromatography and/or mass spectrometry<sup>37,38,39</sup>. However, these  
108 techniques are time consuming, do not permit high throughput testing and are not predictable of *in vivo*  
109 stability, which is of particular interest for peptide-based drugs because of the ease in synthesizing  
110 modified variants, as compared to small molecules or antibodies. We here set out to design a microtiter  
111 plate-based screening assay that aims to determine the stability of CXCR4 ligands in plasma or serum  
112 as well as whole blood. We took advantage of the fact that most if not all CXCR4 antagonists block  
113 CXCL12 binding by occupying a region formed by the second extracellular loop (ECL2) of CXCR4.  
114 ECL2 is also the binding site of the anti-CXCR4 antibody 12G5<sup>40,41</sup>. Thus, most CXCR4 antagonists  
115 compete with binding of 12G5 to CXCR4-expressing cells which can be measured and quantified by  
116 flow cytometry. We demonstrate that this assay allows a robust and convenient determination of ligand-  
117 receptor pharmacodynamics and to measure the stability of CXCR4 ligands in serum/plasma and even  
118 whole human and mouse blood.

119

120

## 121 Results

122

123 **CXCR4 antagonists compete with 12G5 for binding to CXCR4.** It has previously been demonstrated  
124 that several CXCR4 antagonists, including AMD3100<sup>42,43</sup>, EPI-X4<sup>31</sup>, T140<sup>44</sup>, T134<sup>45</sup>, ALX40-4C<sup>46</sup>, and  
125 POL3026<sup>47</sup> compete with the monoclonal anti-CXCR4 12G5 antibody for binding to CXCR4. To  
126 corroborate and expand these findings, several small molecules and peptide-based CXCR4 antagonists  
127 (Table 1) were analyzed for competition with 12G5. As shown in Fig. 1a, all small molecules (with the  
128 exception of MSX-122) resulted in a concentration-dependent reduction of 12G5 binding. IT1t and  
129 Burixafor competed most efficiently with 12G5, with IC<sub>50</sub> values of 1.7 and 0.3 nM, respectively,  
130 whereas AMD070 and AMD3100 were slightly less active (IC<sub>50</sub> values of 37 and 578 nM, respectively)  
131 (Table 2). MSX-122, a partial CXCR4 antagonist did not interfere with 12G5 binding, which is likely  
132 due to the fact that it does not bind to ECL2 but rather penetrates into the deep binding pocket in  
133 CXCR4<sup>20</sup>. In addition, all peptidic antagonists analyzed reduced 12G5 antibody binding in a  
134 concentration-dependent manner. Here, the optimized EPI-X4 derivative WSC02, the respective dimeric  
135 analog WSC02x2, and LY2510924 were most active (IC<sub>50</sub> values of 290, 182 and 151 nM, respectively),  
136 followed by BTK-140, endogenous EPI-X4 and CTCE9908 (Fig. 1b, Table 2). None of the compounds  
137 interfered with binding of the 1D9 antibody, which recognizes the N-terminal flexible domain of  
138 CXCR4 (Fig. S1a and b). BTK140 seemed to reduce 1D9 binding, but this could be attributed to  
139 cytotoxic effects caused by this compound at concentrations above 10 μM (Fig. S1c). Thus, all assayed  
140 CXCR4 ligands (except the partial antagonist MSX-122) prevent binding of the 12G5 antibody.

141

142  
143  
144  
145  
146  
147  
148  
149  
150  
151  
152  
153  
154  
155  
156  
157  
158  
159  
160  
161  
162  
163  
164  
165  
166  
167  
168  
169  
170  
171  
172  
173  
174  
175  
176  
177  
178  
179  
180  
181  
182  
183  
184  
185  
186  
187  
188  
189

**CXCR4 antagonists inhibit CXCR4-tropic HIV-1 infection and block CXCL12-dependent cell migration.** To analyze the CXCR4 ligands in functional assays, we determined their activity against CXCR4 tropic HIV-1 in TZM-bl reporter cells. All small molecule CXCR4 ligands (except MSX-122) suppressed HIV-1 infection with  $IC_{50}$  values in the range of 6 nM for IT1t and 77 nM for Burixafor (Fig. 1c, Table 2). Similarly, all peptide antagonists (except for CTCE-9908) blocked viral infection (Fig. 1d, Table 2), with LY25110924 being the most potent inhibitor ( $IC_{50}$  of 8 nM), followed by WSC02x2 (204 nM) and BTK-140 (293 nM), WSC02 (279 nM) and endogenous EPI-X4 (31  $\mu$ M). Finally, we determined the  $IC_{50}$  of the CXCR4 ligands in antagonizing SupT1 T cell migration towards CXCL12. All tested CXCR4 ligands suppressed migration (except MSX-122). For small molecules we obtained  $IC_{50}$  values between 60 nM (AMD3100) and 1400 nM (Burixafor) (Fig. 1e, Table 2), and for peptides 66 nM for LY2510924, and 15  $\mu$ M for WSC02 (Fig. 1f, Table 2). Thus, with the exception of MSX122 and CTCE-9908, all analyzed CXCR4 ligands bind CXCR4, prevent 12G5-antibody binding, CXCL12-induced cellular migration and X4-tropic HIV-1 infection.

**Determination of  $K_i$  values for CXCR4 ligands.** The Cheng-Prusoff transformation (see formula 3 in material/methods section)<sup>48</sup> was used for calculation of equilibrium inhibition constants ( $K_i$ ) from  $IC_{50}$  values. To ensure that an equilibrium between ligand and antibody is established under the experimental conditions of the antibody competition assays, we first determined  $IC_{50}$ ,  $IC_{90}$  and areas under the curves (AUC) values for EPI-X4 WSC02 after different incubation times. No significant differences were obtained for these values after 1, 2 and 4 hours, showing that an equilibrium was established in the competition assay (Fig. S2). Consequently, all subsequent experiments were performed with a 2-hour incubation period. Since the Cheng-Prusoff transformation requires knowledge of the dissociation constant ( $K_d$ ) of the competing ligand, we experimentally determined the  $K_d$  of the antibody by establishing a saturation binding curve under equilibrium conditions (for reference see <sup>49, 25</sup>). For this, a defined number of 5,000 SupT1 cells per well was incubated with increasing concentrations of the labelled 12G5 antibody, until saturation was reached ( $B_{max}$ ) (Fig. 2a). To exclude unspecific binding, the same experiment was performed in the presence of a high concentration of an optimized EPI-X4 variant (2000  $\mu$ M, >10,000-fold its  $IC_{50}$ ) (Fig. 2a). The unspecific binding signal was then subtracted to obtain values for the specific binding curve. Fig. 2b shows the specific binding curve summarized for 4 individual titrations. From this curve, the half maximal binding concentration  $[Ab]_{0.5}$  of the antibody was determined as 155.5 pM (Fig. 2b, Table S1). Since the  $K_d$  is dependent on the total receptor concentration ( $R_t$ ) used for the reaction, we next quantified surface CXCR4 per cell using quantitative flow cytometry. SupT1 cells were incubated with the 12G5 mAb in saturation. Afterwards cells were stained with labelled secondary antibodies and simultaneously with FACS beads harboring known mAb concentrations. Mean fluorescence (MFI) signals of the beads (Fig. 2c) were used to define a standard curve (Fig. 2d) with that the MFI signal of the cells was interpolated. This approach allowed to calculate in average ~ 29,000 CXCR4 molecules per SupT1 cell, that fit with published data<sup>50</sup>. Based on the total receptor concentration in the assay we then applied formulas 1 and 2 (see methods) to calculate the  $K_d$  of the 12G5 mAb with 151.5 pM (Table S1). Notably,  $IC_{50}$  values obtained for CXCR4 antagonists in competition assay performed with a 10-fold increased number of cells ( $5 \times 10^4$ ) did not change significantly, suggesting that the assay yields robust data even over a broad range of cell numbers (Fig. S3). Next,  $K_i$  values were calculated for all CXCR4 ligands according to formula 3 (Table 2), based on the  $IC_{50}$  values obtained in the competition assays, revealing e.g. sub-nanomolar  $K_i$  values for the small molecules TG-0054 (0.1 nM) and IT1t (0.6 nM) and mostly nanomolar  $K_i$  values for the remaining CXCR4 ligands (Table 2). Thus, the CXCR4 competition assay can be conveniently performed in a microtiter format and allows rapid and quantitative determination of ligand receptor pharmacodynamics.

190 **Adaption of the competition assay to determine plasma stability of CXCR4 ligands.** We were  
191 wondering whether this assay may also allow determining the stability of CXCR4 ligands, in particular  
192 peptides, in human blood plasma. First, we analyzed whether plasma alone (pooled from 6 donors)  
193 interferes with 12G5 binding to CXCR4. As shown in Fig. 3a, a cell culture concentration of 50 %  
194 plasma did not affect antibody binding. Next, we studied proteolytic inactivation of the EPI-X4 WSC02  
195 derivative in plasma. For this, the peptide was diluted in 99.3 % plasma to 20  $\mu$ M and mixtures were  
196 agitated at 37°C. At different time points (minutes to hours), aliquots were taken, serially diluted and  
197 then analyzed in the competition assay (Fig. 3b). We observed a concentration-dependent and complete  
198 suppression of 12G5 binding by WSC02 samples that were taken and analyzed at  $t = 0$  min. Samples  
199 obtained at later time points gradually lost their “function” of blocking antibody binding, which is likely  
200 due to proteolytic inactivation of the peptide in plasma (Fig. 3b). In fact, addition of L-leucinethiol, an  
201 inhibitor of leucyl aminopeptidases that inactivate EPI-X4<sup>31,34</sup>, largely prevented WSC02 inactivation  
202 in plasma (Fig. S4). Of note, even after 24 hours of incubation, WSC02 remained partially active and  
203 competed with 12G5 binding.

204 The time point where the peptide has lost half of its antibody-blocking activity was defined as its half-  
205 life. For its determination, we calculated the fold-change of the  $IC_{50}$  values for the individual time points  
206 relative to the 0 min control (Fig. 3c). The CXCR4 binding activity before incubation was then defined  
207 as 100% and the decay in receptor-binding activity calculated and plotted over time (Fig. 3d). The half-  
208 life ( $t_{1/2}$ ) of WSC02 in plasma was then calculated using a one-phase decay model and revealed a value  
209 of  $\sim 10$  min (Fig. 3d). As an alternative way to determine plasma stability, we considered the individual  
210 areas under the curve (AUCs) values rather than the  $IC_{50}$  values. Similar curve shapes and decay curves  
211 (Fig. 3e, f) and identical average half-lives were determined by both methods, validating both models.  
212 Thus, the 12G5 competition assay allows a rapid and convenient determination of peptide activity in  
213 100% human plasma.

214  
215 **Plasma stability of EPI-X4 derivatives.** Next, we determined plasma stabilities of small molecules  
216 AMD3100 and IT1t or several EPI-X4 derivatives. All compounds (20  $\mu$ M) were resuspended  
217 simultaneously in 100% pooled human plasma, and mixtures were incubated at 37°C. Aliquots were  
218 taken and analyzed essentially as described above. All CXCR4 antagonists obtained at  $t = 0$  blocked  
219 12G5 binding in a concentration-dependent manner (Fig. 4a, 4b). However, peptide-based ligands lost  
220 antibody-competing activity over time (Fig. 4b, Fig. S5) whereas AMD3100 and IT1t remained fully  
221 active, even after 24 h and, in the case of AMD3100, 48 h of incubation (Fig. 4a). The extrapolated and  
222 calculated  $t_{1/2}$  for EPI-X4 was 23 min (Fig. 4a, Fig. S5), confirming previous data obtained with an EPI-  
223 X4 specific sandwich ELISA<sup>31,51</sup>. The improved EPI-X4 derivative WSC02 was less stable ( $t_{1/2}$  of 10  
224 min) (Fig. Fig. 4b, Fig. S5), perhaps because of the L1I exchange at the N-terminus<sup>31</sup>. However, the  
225 corresponding dimer in which two WSC02 molecules are linked via a -S-S- bridge was 19-fold more  
226 stable ( $t_{1/2}$  of 193 min) (Fig. 4b, Fig. S5), suggesting that dimerization prevents the accessibility of the  
227 N-terminal Ile residues for leucyl-aminopeptidases. We then analyzed whether storage of plasma may  
228 affect its proteolytic activity. We found that plasma that was stored at 37°C showed reduced WSC02  
229 inactivating activity (Fig. S6). These results indicate that i) plasma which was obtained and stored under  
230 ill-defined conditions should not be used for stability assays, and ii) that meaningful data can only be  
231 produced within the first 20 h.

232  
233 Next, we evaluated whether the competition assay may be applied to measure peptide degradation in  
234 mouse plasma. EPI-X4 WSC02 was incubated in 100 % human (pooled) and mouse plasma (obtained  
235 from a single animal) for up to 60 min. Mouse plasma alone did not affect 12G5 binding at concentration  
236 of up to 50 % in cell culture, similar as human plasma (Fig. S8a). Loss of CXCR4 binding activity for  
237 EPI-X4 WSC02 was observed for the incubation in both plasma (Fig. S8b), with a more rapid

238 inactivation of the peptide in mouse plasma (Fig. S8c), likely reflecting the increased proteolytic activity  
239 in rodents versus humans.

240

241

242 **Whole blood stability of CXCR4 ligands.** Measuring the stability of drugs in plasma not necessarily  
243 reflects the real conditions in whole blood. To test whether the competition assay performs in blood, we  
244 used fresh EDTA blood obtained from an individual donor. To allow comparison between blood and  
245 plasma, half the of the blood sample was centrifuged to obtain plasma. The different CXCR4 ligands  
246 were diluted to 20  $\mu$ M in both fluids, samples were agitated at 37°C, aliquots taken and frozen at -80°C.  
247 To check for unspecific effects, plasma and blood alone were incubated. Samples were thawed in  
248 parallel, centrifuged to get rid of cells and debris, and simultaneously analyzed for CXCR4 12G5 mAb  
249 competition. Whole blood at concentrations of up to 50 % in cell culture did not interfere with 12G5  
250 binding (Fig. 5a), similar to plasma (Fig. 3a and 5a). As observed in the experiment before with pooled  
251 plasma, IT1t was moderately impaired in its ability to block 12G5 binding upon incubation in plasma  
252 derived from the individual donor as well as whole blood (Fig. 5b), and AMD3100 remained fully active  
253 even after 24 h (Fig. 5c). Notably, both WSC02 (Fig. 5d) and its dimer WSC02x2 (Fig. 5e) were less  
254 stable in blood compared to plasma.

255

## 256 DISCUSSION

257

258 Antibody competition assays have long been used to study the interaction of ligands with receptors, e.g  
259 chemokine receptors<sup>52,53,25,54</sup>. There are several advantages in using antibodies instead of chemokine  
260 ligands for these kinds of assays. On the one hand, chemokines are the natural receptor ligands and  
261 therefore of high physiological relevance. On the other hand, they often have the disadvantage of being  
262 not specific for only one receptor<sup>55</sup>. CXCL12 for example, the natural chemokine ligand for CXCR4,  
263 also binds with high affinity to CXCR7 making it necessary to test all cells for expression of this receptor  
264 beforehand<sup>56</sup>. Antibodies are usually very specific for their target and can therefore be used on any  
265 desired cell type. Also, chemokines perform a two-step binding mode<sup>57</sup>. They first bind to the N-  
266 terminus of the GPCR and afterwards to the orthosteric binding pocket. If a small molecule blocks  
267 binding to the orthosteric binding site, it could happen that the labelled chemokine still “sticks” to the  
268 N-terminus of the receptor. This effect was, for example, demonstrated for CXCL12 that could not  
269 completely be released from CXCR4 upon binding of AMD3100<sup>58</sup>. This might lead to a background  
270 signal during the FACS measurement<sup>54</sup>. Another very important point is that chemokine binding leads  
271 to cell signaling and often to internalization. Background signal caused by internalized fluorescent  
272 ligand can be minimized by using an antibody, that does not lead to internalization of the receptor.  
273 Also, labelled chemokines are comparably more expensive than most antibodies, what limits the  
274 throughput of such assays especially in smaller laboratories. For those reasons, we here describe a  
275 competition binding assay based on a fluorescently labelled antibody that allows the rapid determination  
276 of binding affinities of CXCR4 antagonists *in vitro* and its adaption to determine stability of ligands in  
277 human or mouse blood *ex vivo*.

278 A prerequisite for this assay is that ligand and antibody share orthosteric binding sites on the receptor,  
279 resulting in a competitive binding mode. Because of its importance as drug target, CXCR4 is a well-  
280 researched receptor, and a variety of antibodies targeting different epitopes on CXCR4 exist. The  
281 monoclonal antibody 12G5 binds a region in the second extracellular loop 2 (ECL2) of CXCR4, and  
282 competitively abrogates binding by the chemokine ligand CXCL12<sup>40,41,59</sup>. Similarly, antibody  
283 competition assays with 12G5 demonstrated that ECL2 serves as binding site for many CXCR4  
284 antagonizing compounds that are currently in (pre)clinical development.

285

286 We here confirm these data and show that all analyzed peptides (BKT140, CTCE-9908, LY2510924,  
287 EPI-X4 and its optimized derivative) and small molecule (AMD3100, AMD070, IT1t, TG-0054)  
288 inhibitors of CXCR4 compete with 12G5 binding. The only exception was MSX-122, a biased CXCR4  
289 ligand that intervenes in the  $G\alpha_i$ -signaling pathway (cAMP modulation), but not the  $G_q$ -pathway  
290 (calcium flux)<sup>20</sup>. Interestingly, molecular docking experiments suggested that MSX-122 binds in close  
291 proximity to a spacious pocket in CXCR4 that is also occupied by BTK140. MSX-122 (292 Da) is the  
292 smallest of all tested compounds and binds near the bottom of the binding pocket<sup>20</sup>. BTK140 (2159 Da)  
293 is 7 times larger but displaced 12G5, suggesting that MSX-122 is simply too small to interfere with  
294 12G5 binding to ECL2. In agreement with this assumption are previous studies reporting that MSX-122  
295 is not preventing CXCL12 binding, and our data presented here that MSX-122 is not affecting CXCR4-  
296 tropic HIV-1 infection, in contrast to most other tested CXCR4 antagonists.

297  
298 The fluorescence-based antibody competition assay allows for a rapid and quantitative determination of  
299 the half-maximal inhibitory concentration ( $IC_{50}$ ) and the inhibitory constants ( $K_i$ ) for each CXCR4  
300 ligand analyzed, allowing a direct comparison of pharmacological parameters. The lowest  $K_i$ , (~ 0.1  
301 nM) was observed for Burixafor (TG-0054), an orally bioavailable stem cell mobilizing agent currently  
302 in phase I trials<sup>23</sup>, followed by IT1t ( $K_i$  ~ 0.6 nM), an allosteric inhibitor that is currently not in clinical  
303 development. AMD3100, the only marketed CXCR4 antagonist approved to mobilize hematopoietic  
304 stem cells in cancer patients<sup>60</sup> and currently also in advanced clinical trials for therapy of other CXCR4-  
305 associated diseases, showed a high nanomolar  $K_i$  with 221 nM. For peptide-based drugs, the lowest  $K_i$   
306 value was obtained for the cyclic LY251092 which is in phase I and II as part of a combination therapy  
307 against cancer. The dimeric EPI-X4 derivative WSC02x2 showed a  $K_i$  of 69 nM, which is ~10-fold  
308 lower than that of the endogenous peptide and reflects also its enhanced potency in inhibiting CXCR4-  
309 tropic HIV-1 infection and CXCL12-dependent cell migration. Due to the high assay performance  
310 (quick and easy) we are currently applying the 12G5 competition assay in an ongoing QSAR study with  
311 more than 200 EPI-X4 analogs in order to identify leads with reduced  $K_i$  values for further preclinical  
312 development.

313  
314 The greatest advantage of the assay is to quickly and accurately determine the *functional* stability of  
315 CXCR4 ligands in plasma and whole blood by measuring the *activity* (competition with 12G5 for  
316 binding to CXCR4) rather than physical *presence* of the drugs. From the availability of the samples until  
317 the completion of the analysis by flow cytometry and evaluation of the data, it only takes 3 hours per 96  
318 well plate. Furthermore, no sample processing is required as the peptide-containing specimen  
319 (plasma/blood) is applied directly to the cells together with the antibody. This is in sharp contrast to all  
320 other approaches, mainly mass spectrometry-based (MS) methods, that directly quantify the presence  
321 (or absence) of the analyte. These measures are time consuming and labor intensive, as the analyte  
322 containing plasma/blood sample first has to be processed to extract peptides/proteins, followed by  
323 chromatographic separation and quantitative MS, which often requires additional internal standards and  
324 expensive equipment and experienced operators. Furthermore, the antibody-based assay also allows to  
325 quantify receptor-binding of CXCR4 ligands that are bound to plasma proteins (data not shown), which  
326 may otherwise not be detected by MS. For example, 58% of administered AMD3100 directly binds to  
327 plasma proteins including albumin<sup>61,62</sup> and may be missed by MS analysis.

328  
329 Another advantage of the 12G5 antibody competition assay is that it enables analysis of peptide  
330 stability/activity not only in human plasma or blood but also in the respective body fluids from mice.  
331 Mouse models are normally the first choice to determine toxicity, pharmacokinetic and  
332 pharmacodynamic parameters of drugs *in vivo*, and usually involve killing the animals. Our assay  
333 precedes *in vivo* experiments and allows to identify candidates that are rapidly degraded (or even

334 cytotoxic) prior to the animal studies. Thus, these candidate drugs will be eliminated from further  
335 analysis, which should substantially reduce animal numbers. Moreover, based on the stability profiles  
336 obtained *in vitro*, we may have first predictive values for doses to be applied later *in vivo*.

337  
338 The competition assay is particularly useful when studying the stability of drug candidates that are prone  
339 to inactivation or degradation in blood, such as peptides. Our results obtained herein for the plasma half-  
340 life of the peptide inhibitor EPI-X4 ( $t_{1/2}$  23 min) largely confirm those previously obtained using an EPI-  
341 X4 sandwich ELISA (17 min)<sup>31</sup>. We also corroborate that leucyl aminopeptidases are responsible for  
342 EPI-X4 degradation in plasma<sup>31</sup>, because addition of an inhibitor of these enzymes decreased proteolytic  
343 inactivation. The optimized derivative WSC02 was shown to have a  $t_{1/2}$  of 10 min in plasma and 9 min  
344 in blood. Interestingly, the dimeric version coupled through a disulfide bridge, WSC02x2, showed  
345 increased stability (or resistance to proteolytic inactivation) with  $t_{1/2}$  in plasma of greater than 3 h and  
346 in blood of 80 min. This finding suggests that dimerization may protect the N-terminal Isoleucine  
347 residues from efficient recognition or proteolysis by leucyl aminopeptidases. Thus, the 12G5  
348 competition assay not only enables to determine binding affinities of EPI-X4 derivatives but also to  
349 quickly measure peptide stability in mouse and human blood, and is now routinely used as gold assay  
350 in advanced SAR studies that aim to generate highly active and stable EPI-X4 derivatives.

351

352

## 353 **METHODS**

354

### 355 **Reagents**

356 CTCE-9908 (#5130), and IT1t (#4596) was obtained from Tocris, Burixafor was obtained from MedKoo  
357 Biosciences (#206522), AMD070 (#HY-50101A), MSX-122 (#HY-13696), BKT-140 (#HY-P0171),  
358 and LY2510924 (#HY-12488) was obtained from Hycultec, AMD3100 octahydrochloride hydrate  
359 was obtained from Sigma-Aldrich (#A5602). Substances were diluted at a stock concentration of 10  
360 mM. EPI-X4 and WSC02 were synthesized automatically on a 0.10 mmol scale using standard Fmoc  
361 solid phase peptide synthesis techniques with the microwave synthesizer (Liberty blue; CEM). Amino  
362 acids were obtained from Novabiochem (Merck KGaA, Darmstadt, Germany). Peptides were purified  
363 using reverse phase preparative high-performance liquid chromatography (HPLC; Waters) in an  
364 acetonitrile/water gradient under acidic conditions on a Phenomenex C18 Luna column and afterwards  
365 lyophilized on a freeze dryer (Labconco). Prior to use peptides were diluted in PBS at a stock  
366 concentration of 3 mM. Recombinant human SDF-1 $\alpha$  (CXCL12) was obtained from Peprotech and  
367 reconstituted at 100  $\mu$ g/mL in water. WSC02-dimer (WSC02x2) was prepared by on-air-oxidation of  
368 the monomer via disulfide bonds at the cysteines in aquatic solution (pH 8.0) at 1 mg/mL peptide  
369 concentration. The dimerized peptide was then chromatographically purified and freeze dried. APC  
370 mouse anti-human CD184 (clone 12G5; #555976) and PE rat anti-human CD184 (clone 1D9; #551510)  
371 and the appropriate isotype controls were obtained from BD Pharmingen™. L-leucinethiol (LAP) was  
372 obtained from Sigma Aldrich (#L8397).

### 373 **Blood and blood plasma**

374 Whole blood was collected from healthy donors in EDTA tubes and directly used or subsequently  
375 centrifuged for 15 min at 2,500 x g to obtain plasma. Plasma from 6 donors was pooled and stored in  
376 aliquots at -80°C. Mouse plasma was obtained by heart punctation of BL6 mice after cervical  
377 dislocation. Blood was 19:1 diluted with 0.16 M NaEDTA and centrifuged at 2000 rcf for 20 min at 4°C  
378 to obtain plasma.

### 379 **Statement**



380 All experiments and methods were performed in accordance with relevant guidelines and regulations.  
381 All experimental protocols were approved by a named institutional/licensing committee. Experiments  
382 involving human blood and plasma were reviewed and approved by the Institutional Review Board (i.e.,  
383 the Ethics Committee of Ulm University). Informed consent was obtained from all human subjects. All  
384 human-derived samples were anonymized before use. All animal experiments were performed in  
385 accordance with the Directive 2010/63/EU of the European Parliament and approved by the regulatory  
386 authority of the state of Baden-Württemberg and in compliance with German animal protection laws.

### 387 **Cell culture**

388 TZM-bl HIV-1 reporter cells stably expressing CD4, CXCR4 and CCR5 and harboring the lacZ reporter  
389 genes under the control of the HIV LTR promoter were obtained through the NIH AIDS Reagent  
390 Program, Division of AIDS, NIAID, NIH: TZM-bl cells (Cat#8129) from Dr. John C. Kappes, and Dr.  
391 Xiaoyun Wu. TZM-bl cells and HEK293T cells were cultured in DMEM supplemented with 10 % fetal  
392 calf serum (FCS), 100 units/mL penicillin, 100 µg/mL streptomycin, and 2 mM L-glutamine (Gibco).  
393 SupT1 cells were cultured in RPMI supplemented with 10% FCS, 100 units/mL penicillin, 100 µg/mL  
394 streptomycin, 2 mM L-glutamine and 1 mM HEPES (Gibco).

### 395 **HIV-1 inhibition assay**

396 Viral stocks of CXCR4-tropic NL4-3 were generated by transient transfection of 293T cells with  
397 proviral DNA as described<sup>63</sup>. The next day the transfection mixture was removed and fresh medium  
398 containing 2.5 % FCS was added. 2 days after transfection the supernatant was harvested and cell debris  
399 were removed by centrifugation. Aliquots were stored at -80°C. For infection of TZM-bl cells in  
400 presence of inhibitors, cells were seeded at a density of  $1 \times 10^5$  in 70 µL DMEM containing 2.5 % FCS.  
401 Compounds were diluted in PBS and 10 µL were added. After 15 min of incubation cells were inoculated  
402 with 20 µL of diluted virus. Infection rates were determined three days after using Gal-Screen system  
403 (Applied Biosystems).

### 404 **Cell migration**

405 Migration Assays were performed using 96-well transwell assay plates (Corning Incorporated,  
406 Kennebunk, ME, USA) with 5 µm polycarbonate filters. First, 50 µl ( $0.75 \times 10^5$ ) of SupT1 cells  
407 resuspended in assay buffer (RPMI supplemented with 0.1 % BSA) were added into the upper chamber  
408 together with/without the compounds and allowed to settle down for around 15 min. In the meanwhile,  
409 200 µl assay buffer with or without 100 ng/ml CXCL12 were filled into a 96 well-V plate. To avoid  
410 diffusion of the compounds from the upper to the lower compartment compounds were added in the  
411 same concentrations to the lower chamber. Next, the upper chamber was placed onto the 96 well-V plate  
412 and cells were allowed to migrate towards CXCL12 for 4 h at 37°C (5 % CO<sub>2</sub>). Afterwards, migrated  
413 cells in the lower compartment were directly analyzed by Cell-Titer-Glo® assay (Promega, Madison,  
414 WI, USA). The percentage of migrated cells was calculated as described by Balabanian et al (2005)<sup>64</sup>.  
415 To determine the relative migration in %, the percentage of migrated cells was normalized to the  
416 CXCL12 control without inhibitors.

### 417 **Quantitative flow cytometry**

418 CXCR4 levels on SupT1 cells were determined using QIFIKIT® (Agilent Dako) according to the  
419 manufacturer's protocol. Shortly, SupT1 cells were labelled with a primary CXCR4 antibody (clone  
420 12G5) at a saturating concentration. Then the cells in parallel with provided beads coated with defined  
421 quantities of a mouse monoclonal antibody are incubated with a fluorescently labelled secondary  
422 antibody and analyzed by flow cytometry. The mean fluorescence of the cells was then interpolated with  
423 the bead's calibration curve.

### 424 **Antibody competition assay**

425 Competition of compounds with antibody binding was performed on SupT1 cells. For that cells were  
426 washed in PBS containing 1 % FCS by centrifugation (1.300 rpm, 4°C) and 5,000 cells (for  $K_i$   
427 determinations) or 50,000 cells were then seeded per well in a 96 V-well plate. Buffer was removed by  
428 centrifugation and plates were precooled at 4°C for at least 15 min. Compounds were serially diluted in  
429 ice cold PBS and 12G5-APC antibody was diluted in cold PBS containing 1 % FCS. 15  $\mu$ L of  
430 compounds was then added to the cells and 15  $\mu$ L antibody immediately afterwards (0.245 nM final  
431 concentration). Plates were incubated at 4°C in the dark for 2 hours. Afterwards cells were washed twice  
432 by centrifugation with PBS containing 1 % FCS and fixed with 2 % PFA. During all pipetting steps,  
433 plates were kept cool by using a cooling pad. Antibody binding was analyzed by flow cytometry (FACS  
434 CytoFLEX; Beckman Coulter®) by determination of the mean fluorescence intensity (MFI) of at least  
435 5.000 cells (50.000 cells per well) or 1.000 cells (5.000 cells per well).

436

### 437 **Formulas**

438

439  $K_d$  calculation for 12G5

440 (1)  $K_d = [Ab]_{0.5} - \frac{[Rt]}{2}$

441 For  $[Ab]_{0.5}$  = concentration where free ligand  $[L]$  is  $K_d$

442  $K_d$  = dissociation constant

443  $R_t$  = total receptor concentration; so:

444 (2)  $K_d = 155.5 - 8 \text{ pM} \times 0.5 = 151.5 \text{ pM}$

445  $K_i$  calculation

446 (3)  $K_i = \frac{IC_{50}}{(1 + \frac{[L]}{K_d})}$

447 For  $K_i$  = inhibitory constant

448  $IC_{50}$  = half maximal inhibition for 12G5 binding

449  $[L]$  = 12G5 concentration

450  $K_d$  = dissociation constant of 12G5

451

452

### 453 **Stability measurements in whole human plasma or blood**

454 Compounds were 150-fold diluted in human plasma or whole human blood to reach final concentrations  
455 of 20  $\mu$ M. The  $t = 0$  sample was immediately taken and stored at -80°C. Plasma/compound or  
456 blood/compound mixture was then transferred to 37°C and shook at 350 rpm. At given time points  
457 samples were taken and stored at -80°C°. For measuring the functional activity of the plasma/peptide  
458 samples, the mixtures were thawed and serially diluted in ice cold PBS (starting with 100 % sample).  
459 12G5-APC antibody competition was then performed as described before. Note, that during the  
460 competition process the samples are 1:1 diluted with the antibody and the highest plasma concentration  
461 on cells was 50 %. For blood/peptide functional stability, samples were thawed and centrifuged at 14,000  
462 rpm for 3 min at 4°C to remove cells and debris. The supernatant was then serially diluted in PBS  
463 (starting with 100 % sample) and 12G5-antibody competition assay was performed. After the 2 h  
464 incubation, the cells were washed by centrifugation (1.300 rpm, 4°C) and 50  $\mu$ L of 1-step-Fix/Lyse  
465 solution (Thermo Fisher #00-5333-54) was added for 15 min at room temperature. Afterwards cells  
466 were washed again and analyzed for bound antibody.

### 467 **Calculations and statistical analysis**

468 Statistical analysis was performed in GraphPad Prism (version 8.3.0).  $IC_{50}$  and  $IC_{90}$  curves and the areas  
469 under the curves (AUC) were determined by nonlinear regression. For half-life calculations, the  $IC_{50}$   
470 values for each time point as well as the AUCs were analyzed and normalized relative to  $t = 0$ . Activities  
471 were then determined ( $(IC_{50}(t = 0) / IC_{50}(t)) \times 100$ ) for each time point and half-lives determined by a  
472 One-Phase-Decay model.

473

## 474 References

- 475 1. Janssens, R. *et al.* Truncation of CXCL12 by CD26 reduces its CXC chemokine receptor 4-  
476 and atypical chemokine receptor 3-dependent activity on endothelial cells and lymphocytes.  
477 *Biochem. Pharmacol.* **132**, 92–101 (2017).
- 478 2. Pawig, L., Klasen, C., Weber, C., Bernhagen, J. & Noels, H. Diversity and Inter-Connections  
479 in the CXCR4 Chemokine Receptor/Ligand Family: Molecular Perspectives. *Front. Immunol.*  
480 **6**, 429 (2015).
- 481 3. Zou, Y.-R., Kottmann, A. H., Kuroda, M., Taniuchi, I. & Littman, D. R. Function of the  
482 chemokine receptor CXCR4 in haematopoiesis and in cerebellar development. *Nature* **393**,  
483 595–599 (1998).
- 484 4. Cavallero, S. *et al.* CXCL12 Signaling Is Essential for Maturation of the Ventricular Coronary  
485 Endothelial Plexus and Establishment of Functional Coronary Circulation. *Dev. Cell* **33**, 469–  
486 477 (2015).
- 487 5. Ara, T., Tokoyoda, K., Okamoto, R., Koni, P. A. & Nagasawa, T. The role of CXCL12 in the  
488 organ-specific process of artery formation. *Blood* **105**, 3155–3161 (2005).
- 489 6. SALCEDO, R. & OPPENHEIM, J. J. Role of Chemokines in Angiogenesis: CXCL12/SDF-1  
490 and CXCR4 Interaction, a Key Regulator of Endothelial Cell Responses. *Microcirculation* **10**,  
491 359–370 (2010).
- 492 7. Nie, Y. *et al.* The Role of CXCR4 in Maintaining Peripheral B Cell Compartments and  
493 Humoral Immunity. *J. Exp. Med.* **200**, 1145–1156 (2004).
- 494 8. Petit, I. *et al.* G-CSF induces stem cell mobilization by decreasing bone marrow SDF-1 and up-  
495 regulating CXCR4. *Nat. Immunol.* **3**, 687–694 (2002).
- 496 9. Choi, W.-T., Duggineni, S., Xu, Y., Huang, Z. & An, J. Drug Discovery Research Targeting  
497 the CXC Chemokine Receptor 4 (CXCR4). *J. Med. Chem.* **55**, 977–994 (2012).
- 498 10. Feng, Y., Broder, C. C., Kennedy, P. E. & Berger, E. A. HIV-1 Entry Cofactor: Functional  
499 cDNA Cloning of a Seven-Transmembrane, G Protein-Coupled Receptor. *Science (80- )*. **272**,  
500 872–877 (1996).
- 501 11. Moore, J. P., Kitchen, S. G., Pugach, P. & Zack, J. A. The CCR5 and CXCR4 Coreceptors—  
502 Central to Understanding the Transmission and Pathogenesis of Human Immunodeficiency  
503 Virus Type 1 Infection. *AIDS Res. Hum. Retroviruses* **20**, 111–126 (2004).
- 504 12. Donzella, G. A. *et al.* AMD3100, a small molecule inhibitor of HIV-1 entry via the CXCR4 co-  
505 receptor. *Nat. Med.* **4**, 72–77 (1998).
- 506 13. Moyle, G. *et al.* Proof of Activity with AMD11070, an Orally Bioavailable Inhibitor of  
507 CXCR4-Tropic HIV Type 1. *Clin. Infect. Dis.* **48**, 798–805 (2009).
- 508 14. Tamamura, H. *et al.* Pharmacophore identification of a chemokine receptor (CXCR4)  
509 antagonist, T22 ([Tyr 5,12, Lys 7]-polyphemusin II), which specifically blocks T cell-line-  
510 tropic HIV-1 infection. *Bioorg. Med. Chem.* **6**, 1033–1041 (1998).
- 511 15. Peng, S.-B. *et al.* Identification of LY2510924, a Novel Cyclic Peptide CXCR4 Antagonist  
512 That Exhibits Antitumor Activities in Solid Tumor and Breast Cancer Metastatic Models. *Mol.*  
513 *Cancer Ther.* **14**, 480–490 (2015).
- 514 16. Ghobrial, I. M. *et al.* A Phase Ib/II Trial of the First-in-Class Anti-CXCR4 Antibody  
515 Ulocuplumab in Combination with Lenalidomide or Bortezomib Plus Dexamethasone in  
516 Relapsed Multiple Myeloma. *Clin. Cancer Res.* **26**, 344–353 (2020).

- 517 17. Jahnichen, S. *et al.* CXCR4 nanobodies (VHH-based single variable domains) potently inhibit  
518 chemotaxis and HIV-1 replication and mobilize stem cells. *Proc. Natl. Acad. Sci.* **107**, 20565–  
519 20570 (2010).
- 520 18. Hendrix, C. W. *et al.* Safety, Pharmacokinetics, and Antiviral Activity of AMD3100, a  
521 Selective CXCR4 Receptor Inhibitor, in HIV-1 Infection. *JAIDS J. Acquir. Immune Defic.*  
522 *Syindr.* **37**, 1253–1262 (2004).
- 523 19. De Clercq, E. *et al.* Highly potent and selective inhibition of human immunodeficiency virus  
524 by the bicyclam derivative JM3100. *Antimicrob. Agents Chemother.* **38**, 668–674 (1994).
- 525 20. Liang, Z. *et al.* Development of a Unique Small Molecule Modulator of CXCR4. *PLoS One* **7**,  
526 e34038 (2012).
- 527 21. Home - ClinicalTrials.gov. Available at: <https://clinicaltrials.gov/ct2/home>. (Accessed: 23rd  
528 April 2020)
- 529 22. Mosi, R. M. *et al.* The molecular pharmacology of AMD11070: An orally bioavailable CXCR4  
530 HIV entry inhibitor. *Biochem. Pharmacol.* **83**, 472–479 (2012).
- 531 23. Setia, G. *et al.* A Phase II, Open-Label Pilot Study to Evaluate the Hematopoietic Stem Cell  
532 Mobilization of TG-0054 Combined with G-CSF in 12 Patients with Multiple Myeloma, Non-  
533 Hodgkin Lymphoma or Hodgkin Lymphoma - an Interim Analysis. *Blood* **126**, 515–515  
534 (2015).
- 535 24. Wu, B. *et al.* Structures of the CXCR4 chemokine GPCR with small-molecule and cyclic  
536 peptide antagonists. *Science* **330**, 1066–1071 (2010).
- 537 25. Rosenkilde, M. M. *et al.* Molecular Mechanism of AMD3100 Antagonism in the CXCR4  
538 Receptor. *J. Biol. Chem.* **279**, 3033–3041 (2004).
- 539 26. Smith, N. *et al.* Control of TLR7-mediated type I IFN signaling in pDCs through CXCR4  
540 engagement—A new target for lupus treatment. *Sci. Adv.* **5**, eaav9019 (2019).
- 541 27. Wong, D., Korz, W., Merzouk, A. & Salari, H. A peptide antagonist of chemokine receptor  
542 CXCR4 reduces tumor metastasis in a murine orthotopic model of human prostate cancer.  
543 *Cancer Res.* **66**, 511 (2006).
- 544 28. Nagler, A. *et al.* BKT140 Is a Novel CXCR4 Antagonist with Stem Cell Mobilization and  
545 Antimyeloma Effects: An Open-Label First Human Trial In Patients with Multiple Myeloma  
546 Undergoing Stem Cell Mobilization for Autologous Transplantation. *Blood* **116**, 2260–2260  
547 (2010).
- 548 29. Comprehensive Cancer Information - National Cancer Institute. Available at:  
549 <https://www.cancer.gov/>. (Accessed: 23rd April 2020)
- 550 30. Tahirovic, Y. A. *et al.* Small molecule and peptide-based CXCR4 modulators as therapeutic  
551 agents. A patent review for the period from 2010 to 2018. *Expert Opin. Ther. Pat.* **30**, 87–101  
552 (2020).
- 553 31. Zirafi, O. *et al.* Discovery and Characterization of an Endogenous CXCR4 Antagonist. *Cell*  
554 *Rep.* **11**, 737–747 (2015).
- 555 32. Müller, J. A., Zirafi, O., Roan, N. R., Lee, S. J. & Münch, J. Evaluation of EPI-X4 as a urinary  
556 peptide biomarker for diagnosis and prognosis of late acute GvHD. *Bone Marrow Transplant.*  
557 **51**, 1137–1139 (2016).
- 558 33. Buske, C., Kirchhoff, F. & Münch, J. EPI-X4, a novel endogenous antagonist of CXCR4.  
559 *Oncotarget* **6**, 35137–35138 (2015).
- 560 34. Zirafi, O., Hermann, P. C. & Münch, J. Proteolytic processing of human serum albumin  
561 generates EPI-X4, an endogenous antagonist of CXCR4. *J. Leukoc. Biol.* **99**, 863–868 (2016).

- 562 35. Kalatskaya, I. *et al.* AMD3100 Is a CXCR7 Ligand with Allosteric Agonist Properties. *Mol.*  
563 *Pharmacol.* **75**, 1240–1247 (2009).
- 564 36. Romero-Molina, S., Ruiz-Blanco, Y. B., Harms, M., Münch, J. & Sanchez-Garcia, E. PPI-  
565 Detect: A support vector machine model for sequence-based prediction of protein-protein  
566 interactions. *J. Comput. Chem.* **40**, 1233–1242 (2019).
- 567 37. Böttger, R., Hoffmann, R. & Knappe, D. Differential stability of therapeutic peptides with  
568 different proteolytic cleavage sites in blood, plasma and serum. *PLoS One* **12**, e0178943  
569 (2017).
- 570 38. Di, L., Kerns, E. H., Hong, Y. & Chen, H. Development and application of high throughput  
571 plasma stability assay for drug discovery. *Int. J. Pharm.* **297**, 110–119 (2005).
- 572 39. Hartman, D. A. Determination of the Stability of Drugs in Plasma. in *Current Protocols in*  
573 *Pharmacology* **Chapter 7**, Unit 7.6 (John Wiley & Sons, Inc., 2003).
- 574 40. Carnec, X., Quan, L., Olson, W. C., Hazan, U. & Dragic, T. Anti-CXCR4 Monoclonal  
575 Antibodies Recognizing Overlapping Epitopes Differ Significantly in Their Ability To Inhibit  
576 Entry of Human Immunodeficiency Virus Type 1. *J. Virol.* **79**, 1930–1933 (2005).
- 577 41. Ray-Saha, S., Huber, T. & Sakmar, T. P. Antibody Epitopes on G Protein-Coupled Receptors  
578 Mapped with Genetically Encoded Photoactivatable Cross-Linkers. *Biochemistry* **53**, 1302–  
579 1310 (2014).
- 580 42. Fricker, S. P. *et al.* Characterization of the molecular pharmacology of AMD3100: A specific  
581 antagonist of the G-protein coupled chemokine receptor, CXCR4. *Biochem. Pharmacol.* **72**,  
582 588–596 (2006).
- 583 43. Li, Z. *et al.* Design, synthesis, and structure-activity-relationship of a novel series of CXCR4  
584 antagonists. *Eur. J. Med. Chem.* **149**, 30–44 (2018).
- 585 44. Tamamura, H. *et al.* A Low-Molecular-Weight Inhibitor against the Chemokine Receptor  
586 CXCR4: A Strong Anti-HIV Peptide T140. *Biochem. Biophys. Res. Commun.* **253**, 877–882  
587 (1998).
- 588 45. Arakaki, R. *et al.* T134, a small-molecule CXCR4 inhibitor, has no cross-drug resistance with  
589 AMD3100, a CXCR4 antagonist with a different structure. *J. Virol.* **73**, 1719–23 (1999).
- 590 46. Doranz, B. J. *et al.* A Small-molecule Inhibitor Directed against the Chemokine Receptor  
591 CXCR4 Prevents its Use as an HIV-1 Coreceptor. *J. Exp. Med.* **186**, 1395–1400 (1997).
- 592 47. Moncunill, G. *et al.* Anti-HIV Activity and Resistance Profile of the CXC Chemokine Receptor  
593 4 Antagonist POL3026. *Mol. Pharmacol.* **73**, 1264–1273 (2008).
- 594 48. Yung-Chi, C. & Prusoff, W. H. Relationship between the inhibition constant (KI) and the  
595 concentration of inhibitor which causes 50 per cent inhibition (I50) of an enzymatic reaction.  
596 *Biochem. Pharmacol.* **22**, 3099–3108 (1973).
- 597 49. Klasse, P. J. *Physicochemical Analyses of the Humoral Immune Response to HIV1 :  
598 Quantification of Antibodies , Their Binding to Viral Antigens and Neutralization of Viral  
599 Infectivity. HIV molecular immunology database 2*, (Los Alamos National Laboratory,  
600 Theoretical Biology and Biophysics, Los Alamos, N.Mex, 1996).
- 601 50. Lee, B., Sharron, M., Montaner, L. J., Weissman, D. & Doms, R. W. Quantification of CD4,  
602 CCR5, and CXCR4 levels on lymphocyte subsets, dendritic cells, and differentially  
603 conditioned monocyte-derived macrophages. *Proc. Natl. Acad. Sci.* **96**, 5215–5220 (1999).
- 604 51. Mohr, K. B. *et al.* Sandwich enzyme-linked immunosorbent assay for the quantification of  
605 human serum albumin fragment 408–423 in bodily fluids. *Anal. Biochem.* **476**, 29–35 (2015).
- 606 52. Hulme, E. C. & Trevethick, M. A. Ligand binding assays at equilibrium: validation and

- 607 interpretation. *Br. J. Pharmacol.* **161**, 1219–1237 (2010).
- 608 53. Maguire, J. J., Kuc, R. E. & Davenport, A. P. Radioligand Binding Assays and Their Analysis.  
609 in *Methods in Molecular Biology* **897**, 31–77 (Humana Press Inc., 2012).
- 610 54. Schoofs, G., Van Hout, A., D’huys, T., Schols, D. & Van Loy, T. A Flow Cytometry-based  
611 Assay to Identify Compounds That Disrupt Binding of Fluorescently-labeled CXC Chemokine  
612 Ligand 12 to CXC Chemokine Receptor 4. *J. Vis. Exp.* **2018**, (2018).
- 613 55. Blanchet, X., Langer, M., Weber, C., Koenen, R. R. & von Hundelshausen, P. Touch of  
614 Chemokines. *Front. Immunol.* **3**, 175 (2012).
- 615 56. Sánchez-Martín, L., Sánchez-Mateos, P. & Cabañas, C. CXCR7 impact on CXCL12 biology  
616 and disease. *Trends in Molecular Medicine* **19**, 12–22 (2013).
- 617 57. Kufareva, I., Salanga, C. L. & Handel, T. M. Chemokine and chemokine receptor structure and  
618 interactions: implications for therapeutic strategies. *Immunol. Cell Biol.* **93**, 372–383 (2015).
- 619 58. Kofuku, Y. *et al.* Structural Basis of the Interaction between Chemokine Stromal Cell-derived  
620 Factor-1/CXCL12 and Its G-protein-coupled Receptor CXCR4. *J. Biol. Chem.* **284**, 35240–  
621 35250 (2009).
- 622 59. Yang, H., Lan, C., Xiao, Y. & Chen, Y.-H. Antibody to CD14 like CXCR4-specific antibody  
623 12G5 could inhibit CXCR4-dependent chemotaxis and HIV Env-mediated cell fusion.  
624 *Immunol. Lett.* **88**, 27–30 (2003).
- 625 60. Plerixafor: AMD 3100, AMD3100, JM 3100, SDZ SID 791. *Drugs R. D.* **8**, 113–9 (2007).
- 626 61. Danner, E., Bonig, H. & Wiercinska, E. Albumin Modifies Responses to Hematopoietic Stem  
627 Cell Mobilizing Agents in Mice. *Cells* **9**, 4 (2019).
- 628 62. European Medicines Agency. *CHMP assessment report for Mozobil.* (2009).
- 629 63. Münch, J. *et al.* Discovery and Optimization of a Natural HIV-1 Entry Inhibitor Targeting the  
630 gp41 Fusion Peptide. *Cell* **129**, 263–275 (2007).
- 631 64. Balabanian, K. *et al.* The Chemokine SDF-1/CXCL12 Binds to and Signals through the  
632 Orphan Receptor RDC1 in T Lymphocytes. *J. Biol. Chem.* **280**, 35760–35766 (2005).
- 633 65. Thoma, G. *et al.* Orally Bioavailable Isothioureas Block Function of the Chemokine Receptor  
634 CXCR4 In Vitro and In Vivo. *J. Med. Chem.* **51**, 7915–7920 (2008).
- 635 66. Chung, D. T. *et al.* TG-0054, a Novel and Potent Stem Cell Mobilizer, Displays Excellent  
636 PK/PD and Safety Profile in Phase I Trial. *Blood* **114**, 866–866 (2009).

637

## 638 **Acknowledgements**

639

640 J.M. and L.S. gratefully acknowledge the German Research Foundation (DFG) for funding the present  
641 study within the CRC1279 framework. J.M. also acknowledges funding through the Baden-  
642 Württemberg Stiftung and the European Research Council.

643

## 644 **Author contributions statement**

645

646 M.H. conceived and conducted all experiments except for the migration assays, carried out by A.G. L.S.  
647 synthesized and analyzed peptides. A.B. and V.R. helped with all mice experiments. C.G. and B.M.  
648 interpreted data and assisted in writing the manuscript. J.M. supervised the study and wrote the paper  
649 together with M.H.

650

## 651 **Competing Interests**

652  
653 A.G., A.B., B.M, V.R. and C.G. declare no competing interest. L.S., M.H. and J.M. are coinventors of  
654 patents claiming the use of EPI-X4 (ALB408-423) and derivatives for the therapy of CXCR4 associated  
655 diseases.

656

657 **Additional Information**

658 Supplementary information accompanies this paper at .....

659

**Figure 1. CXCR4 antibody competition, inhibition of HIV-1 infection, and suppression of T cell migration by CXCR4 ligands.** (a, b) Competition of small molecule (a) and peptide (b) ligands with CXCR4 ECL-2 specific 12G5 antibody. Small molecules and peptides were diluted in PBS and added to SupT1 cells. A constant concentration of APC-labelled 12G5-antibody was added immediately afterwards. After 2 hours incubation in the dark, cells were washed and analyzed by flow cytometry. Data shown are average values derives from 3 individual experiments  $\pm$  SEM. (c, d) Inhibition of HIV-1 infection by CXCR4 ligands. TZM-bl cells were incubated with serial dilutions of compounds for 15 min before they were inoculated with CXCR4-tropic HIV-1. Infection rates were determined after 3 days by  $\beta$ -galactosidase assay. Data shown were derived from 3 individual experiments performed in triplicates  $\pm$  SEM. (e, f) Migration of SupT1 cells in the presence of CXCR4 ligands towards a CXCL12 gradient. The assay was performed in a transwell plate with 5  $\mu$ m pore size with 100 ng/mL CXCL12 in the lower chamber. The number of migrated cells was determined by CellTiterGlo® assay. Shown are average values derived from 3 individual experiments performed in triplicates  $\pm$  SEM.

**Figure 2. Determination of the dissociation constant ( $K_d$ ) of the 12G5-antibody using flow cytometry.** (a) The 12G5-APC antibody was titrated on SupT1 cells. For determination of unspecific binding a CXCR4 antagonist (derivative of WSC02) was applied at its 10,000 fold  $K_d$  during antibody binding and subtracted from the 12G5-binding curve to determine specific antibody binding. Data shown are from one representative experiment. (b) Averaged specific binding curve derived from 4 individual experiments  $\pm$  SEM. (c, d) CXCR4 concentration on SupT1 cells was determined using quantitative flow cytometry. The MFI of SupT1 cells labelled with a primary anti-CXCR4 mouse monoclonal antibody (mAb) and a secondary anti-mouse antibody (c) was compared to a calibration curve derived from bead populations harboring a specific amount of mAb at their surface (d). Shown is one representative experiment.

**Figure 3. Adaption of the antibody competition assay to determine plasma stability of EPI-X4 WSC02.** The peptide (or no peptide as control) was diluted in human plasma (99.3 %) at a concentration of 20  $\mu$ M and incubated at 37°C for 24 h. Aliquots were taken at indicated times and stored at -80°C. Samples were defrosted simultaneously, diluted in PBS, mixed with 12G5-APC antibody and applied to the cells. Bound antibody was analyzed after 2 h of incubation at 4°C by flow cytometry. (a) Plasma alone does not affect 12G5 CXCR4 mAb binding to CXCR4. (b) Antibody inhibition curves obtained at different time points. (c)  $IC_{50}$  values obtained from curves shown in (b) were calculated in GraphPad Prism by non-linear regression and plotted over time. The  $IC_{50}$  obtained at  $t = 0$  was set = 1. (d) Relative CXCR4 binding activity as compared to  $t = 0$ . The half-life was determined by One-phase-decay model using GraphPad Prism. (e) The area under the inhibition curves were determined from data shown in (b) using GraphPad Prism by non-linear regression. AUCs were normalized relative to  $t = 0$ . (f) AUCs were transformed to obtain the activity for given time points relative to  $t = 0$ . Shown are data derived 3 individual incubation rounds using a plasma pool derived from 6 donors  $\pm$  SEM.

**Figure 4. Determination of the functional half-life of CXCR4 ligands in plasma by antibody competition assay.** (a) Small molecules IT1t or AMD3100 or (b) peptides EPI-X4, WSC02, and WSC02x2 were diluted in 99.3 % plasma resulting in 20  $\mu$ M concentrations. Samples were incubated at 37°C, aliquots taken at indicated time points and stored at -80°C. Immediately prior to the competition assay, samples were defrosted, serially diluted in PBS, mixed with 12G5-APC antibody and applied to the cells. Bound antibody was analyzed after 2 h of incubation at 4°C by flow cytometry. The functional half-life ( $t_{1/2}$ ) was determined by calculating the  $IC_{50}$  values of the individual inhibition curves by non-linear regression, which are expressed relative to the  $t = 0$  time point (100 % activity), and applying one-phase-decay model using GraphPad Prism (see Fig. S5). Shown are data derived from three independent rounds of incubation  $\pm$  SEM.

**Figure 5. CXCR4 ligand activity and half-life in whole blood.** No peptide (a), IT1t (b), AMD3100 (c), WSC02 (d) or WSC02x2 (e) were diluted in plasma or whole blood obtained from the same donor. Samples were incubated at 37°C, and aliquots taken and frozen at different time points. Samples were defrosted and centrifuged to remove cells and debris before competition with the 12G5 CXCR4 mAb of all aliquots was done simultaneously as described in Fig. 4. Percent activity was calculated by determining  $IC_{50}$  values for each time point relative to the activity at  $t = 0$  (100%). The half-life was calculated using GraphPad Prism applying a one-phase-decay model (see Fig S. 7). Data shown are derived from an individual experiment.



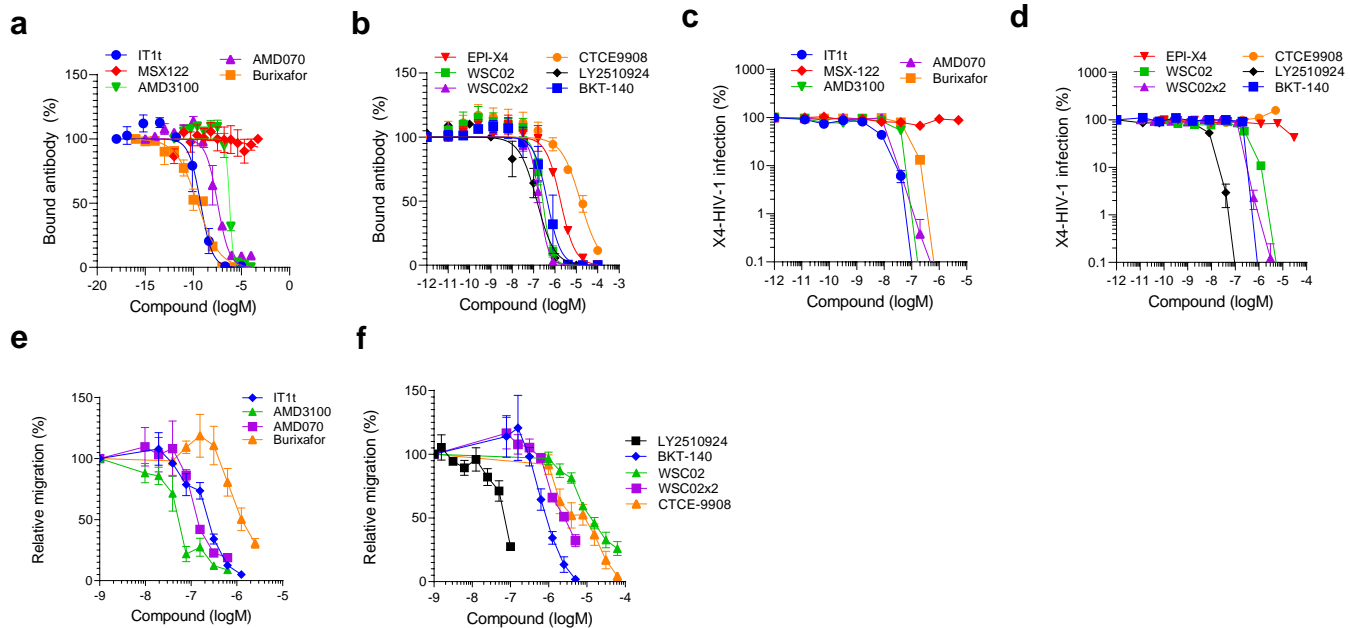
**Table 1. List of the CXCR4 antagonists used in this study.**

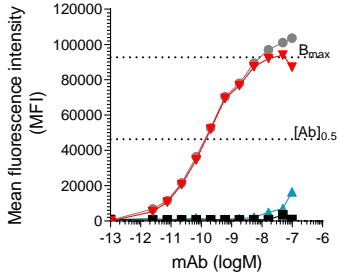
Compound (brand name)	Chemical structure	Molecular weight (Da)	Reference
AMD3100 (Plerixafor)	small molecule	502.8	Clercq et al., 1994 <sup>19</sup>
AMD070 (Mavorixafor)	small molecule	349.5	Moyle et al. 2009 <sup>13</sup>
IT1t	small molecule	479.6	Thoma et al. 2008 <sup>65</sup>
MSX-122	small molecule	292.3	Liang et al. 2012 <sup>20</sup>
TG-0054 (Burixafor)	small molecule	566.7	Chung et al. 2009 <sup>66</sup>
BKT140 (TN14003)	peptide	2159.5	Nagler et al. 2010 <sup>28</sup>
CTCE-9908	peptide	1927.3	Wong et al. 2006 <sup>27</sup>
EPI-X4	peptide	1832	Zirafi et al. 2015 <sup>31</sup>
EPI-X4 WSC02	peptide	1401	Zirafi et al. 2015
EPI-X4 WSC02x2	peptide	2801	Zirafi et al. 2015
LY2510924	cyclic peptide	1189.5	Peng et al. 2015 <sup>15</sup>

**Table 2. Anti-CXCR4 activity and K<sub>i</sub> values of the CXCR4 ligands.**

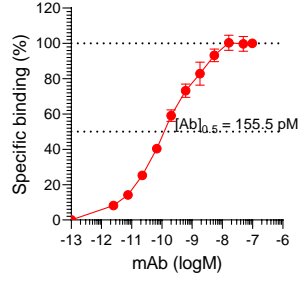
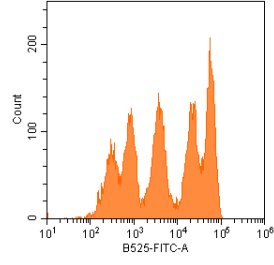
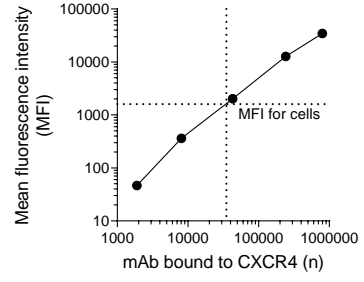
Compound	IC <sub>50</sub> 12G5 (nM) <sup>1</sup>	IC <sub>50</sub> HIV-1 (nM) <sup>2</sup>	IC <sub>50</sub> Migration (nM) <sup>3</sup>	K <sub>i</sub> (nM) <sup>4</sup>
AMD3100	578 ± 105	36 ± 6	60 ± 13	221 ± 40
AMD070	37 ± 15	23 ± 4	152 ± 3	14 ± 6
IT1t	1.5 ± 1	5 ± 0.9	230 ± 20	0.6 ± 0.4
MSX-122	>100,000	>10,000	Nd	-
TG-0054	0.3 ± 0.04	78 ± 6	1401 ± 259	0.1 ± 0.02
BKT-140	508 ± 308	435 ± 153	932 ± 131	194 ± 117
CTCE-9908	16,205 ± 3626	-	6912 ± 2606	6,185 ± 1384
EPI-X4	1,775 ± 162	31,390 ± 3288	Nd	677 ± 62
EPI-X4 WSC02	290 ± 75	257 ± 109	15,824 ± 3502	111 ± 29
EPI-X4 WSC02x2	182 ± 31	254 ± 103	2,672 ± 233	69 ± 12
LY2510924	151 ± 78	8 ± 0.8	66 ± 8	58 ± 30

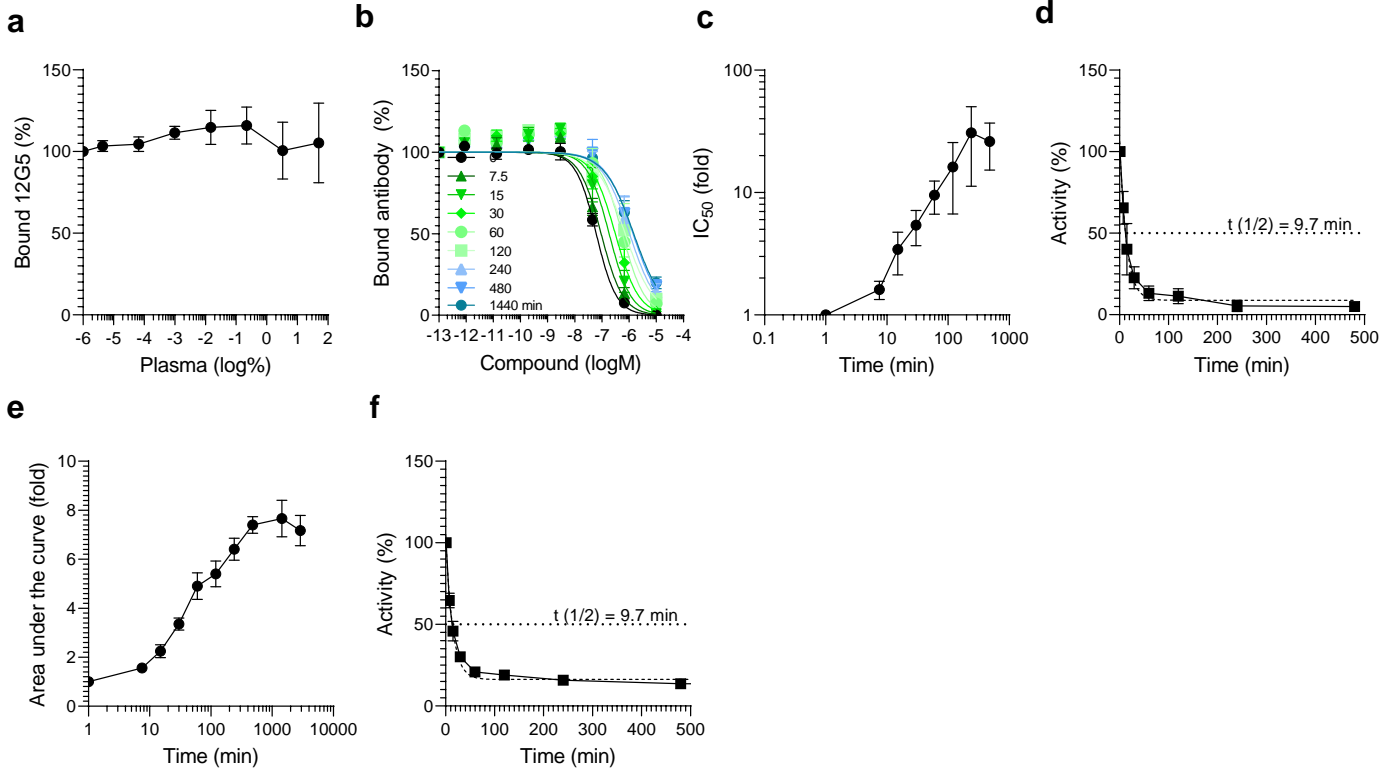
<sup>1</sup> IC<sub>50</sub> shown are means +/- SEM derived from 3 independent 12G5 antibody competition assays. <sup>2</sup> IC<sub>50</sub> shown are mean +/- SEM values obtained from three independent HIV-1 infection assay each performed in triplicates. <sup>3</sup> IC<sub>50</sub> shown are mean +/- SEM values obtained from three independent migration assays each performed in triplicates. <sup>4</sup> K<sub>i</sub> values were calculated as described in the text. Nd = not determined

**Figure 1**

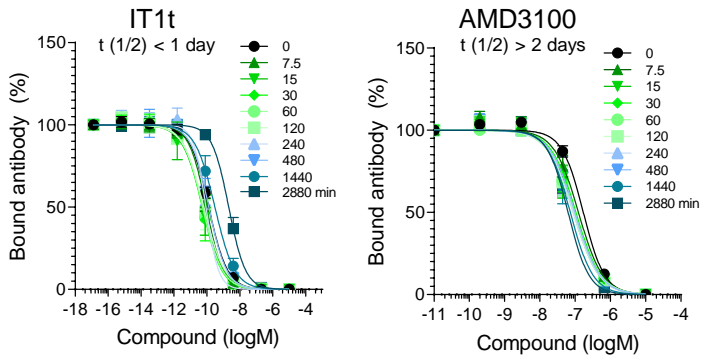
**Figure 2****a**

—▲— specific binding    —▲— 12G5 + CXCR4 antagonist  
—■— isotype control    —●— 12G5

**b****c****d**



a



b

